LETTERS

The breakdown of continuum models for mechanical contacts

Binquan Luan[1] & Mark O. Robbins[1]

Forces acting within the area of atomic contact between surfaces play a central role in friction and adhesion. Such forces are traditionally calculated using continuum contact mechanics[1], which is known to break down as the contact radius approaches atomic dimensions. Yet contact mechanics is being applied at ever smaller lengths, driven by interest in shrinking devices to nanometre scales[2,3], creating nanostructured materials with optimized mechanical properties[3,4], and understanding the molecular origins of macroscopic friction and adhesion[5,6]. Here we use molecular simulations to test the limits of contact mechanics under ideal conditions. Our findings indicate that atomic discreteness within the bulk of the solids does not have a significant effect, but that the atomic-scale surface roughness that is always produced by discrete atoms leads to dramatic deviations from continuum theory. Contact areas and stresses may be changed by a factor of two, whereas friction and lateral contact stiffness change by an order of magnitude. These variations are likely to affect continuum predictions for many macroscopic rough surfaces, where studies[7,8] show that the total contact area is broken up into many separate regions with very small mean radius.

One assumption of continuum mechanics is that the displacements of discrete atoms can be represented by continuously varying strain fields and related to the internal stress by the bulk elastic moduli[1]. There is evidence that this approximation remains surprisingly accurate even at the scale of a few atomic diameters[9–11]. Studies of contact also assume that surfaces are perfectly flat at sufficiently small scales, but the limits of this assumption are rarely considered. As shown below, the atomic structure of surfaces necessarily leads to bumps whose radii of curvature are comparable to an atomic diameter. Moreover, many experiments suggest that macroscopic surfaces become steeper and more curved at smaller length scales[5,7,12]. The applicability of contact mechanics to such surfaces is unclear.

Experimental tests of continuum mechanics in nanometre-scale contacts are difficult. Scanning probe microscopes (SPM) measure total forces and displacements with tips of radius $R \approx 10$–100 nm, but other quantities, such as contact area, must be inferred from friction or conductivity measurements, or estimated from theory[5,13–19]. One motivation of this paper is to quantify the type of errors that may result from such analysis.

We consider geometries that are easy to treat in both continuum theory and atomistic simulations: contact between a rigid cylinder or sphere of radius R and a flat elastic substrate. Within continuum theory this is equivalent to contact between two elastic surfaces[1]. Tests of this equivalence and further details of the simulations are provided in the Supplementary Information.

The substrate is a face-centred cubic (f.c.c.) crystal with a (001) surface, reduced modulus E^*, and volume per atom σ^3, where σ represents an effective atomic diameter. We present results for ideal harmonic crystals, but find similar results for Lennard–Jones interactions (Supplementary Information). Periodic boundary conditions are applied along the surface of the substrate and the bottom is held fixed. For cylinders (Fig. 1) the results are averaged over the spatial period l ($\geq 10\sigma$) along the axis. All other substrate dimensions are much larger ($\geq 200\sigma$), to limit boundary effects.

Three models for the atomic structure of surfaces are considered (Fig. 1). All are identical from the continuum perspective, deviating from a smooth arc by at most σ. The smoothest is a slab of f.c.c. crystal bent into a cylinder. We contrast results for cylinders made by bending crystals with the same atomic spacing as the substrate (commensurate) and an irrational multiple (incommensurate). Amorphous and stepped tips were obtained by cutting cylinders from a bulk glass or crystal. We focus on a radius typical of SPM tips, $R = 100\sigma$ ($\sim$30 nm), but studied R up to $1{,}000\sigma$. Real tip geometries are probably much rougher, but seldom characterized[13]. Atoms on the cylinder and substrate interact with a Lennard–Jones force that, unless noted, is truncated to eliminate adhesion (Supplementary Information).

We first examine the normal tip displacement δ of cylindrical tips as a function of normal force N. Figure 2a shows that results for all surfaces are in quite good agreement with continuum theory[1], even though δ is less than 4σ. Except at very small loads, the main effect of atomic roughness is to uniformly increase δ. This shift represents the difference in height between the lowest atom and a typical atom, and is at most $\sim 0.25\sigma$. Experiments typically include the height at contact ($\delta = 0$) as a fit parameter[17] and Fig. 2a implies that such fits yield accurate values for R and E^* ($\sim$10%).

Figure 2b shows that the errors in contact radius a are greater. Atomic roughness spreads the pressure over a wider region, and the

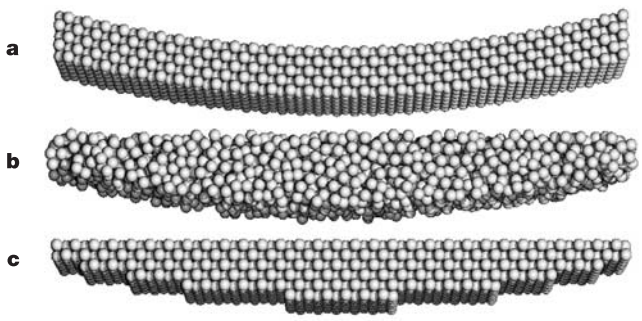

Figure 1 | Cylindrical surfaces with different atomic-scale roughness. Snapshots of atoms near the bottoms of cylindrical surfaces of average radius $R = 100\sigma$ formed by bending a crystalline slab (**a**), or cutting an amorphous (**b**) or crystalline solid (**c**). The steps in **c** are not a unique function of R, which leads to further variations in the behaviour of such tips. The tips are pressed down onto a horizontal elastic substrate. Periodic boundary conditions are applied along the axis of the cylinder, which runs into the page.

[1]Department of Physics & Astronomy, Johns Hopkins University, 3400 N. Charles Streeet, Baltimore, Maryland 21218, USA.

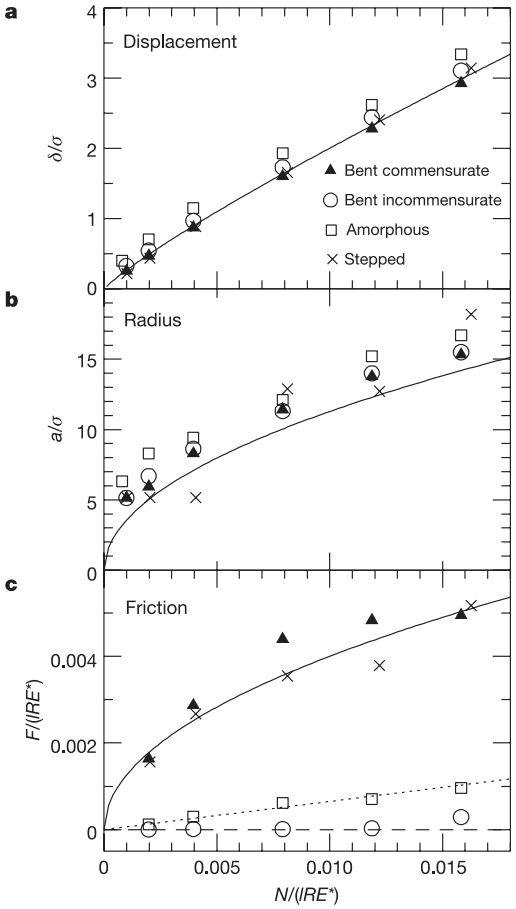

Figure 2 | Variation of normal displacement, contact radius and friction with normal load. Dimensionless plots of normal displacement δ (**a**), contact radius a (**b**) and static friction F (**c**) versus normal force N for the given cylinder surfaces (symbols). For stepped surfaces, a increases in discrete jumps. Here $R = 100\sigma$, the zero of δ corresponds to the first non-zero force, and a is half the range over which the force on substrate atoms is non-zero (Fig. 3). Solid lines show continuum predictions, with the assumption that F is proportional to area in **c**. The broken lines in **c** are linear fits.

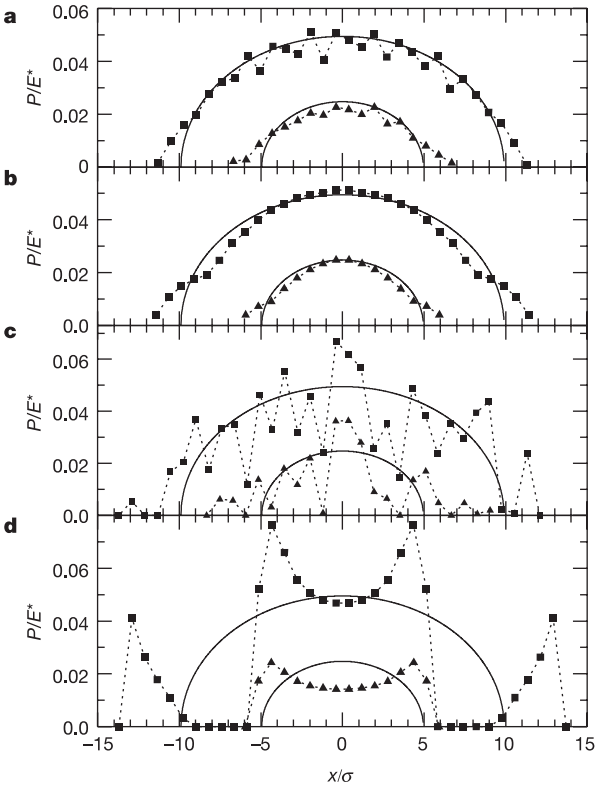

Figure 3 | Local pressure distributions for cylinders with different atomic-scale roughness. Pressure P is plotted as a function of lateral distance x from the cylinder axis for bent incommensurate crystal (**a**), bent commensurate crystal (**b**), amorphous cylinder (**c**), and stepped crystal (**d**). Results for two loads, $N/lRE^* = 0.0019$ (black triangles) and 0.0077 (black squares), are averaged along the length l of the cylinder axis and over bins of width σ along x. Solid lines show continuum predictions for the two loads, which are the same for all panels.

resulting curves cannot be fitted accurately by any fixed values of R and E^*. A better description is provided by increasing the continuum prediction for a by a fixed amount (2 to 5σ) over the whole range of loads. The required increase in a rises with increasing R, doubling by $R = 1{,}000\sigma$. Similar plots are obtained for spherical tips (Supplementary Fig. S2). We conclude that continuum calculations may underestimate the area of SPM contacts by up to 100% at small loads, but that the fractional error decreases with increasing load and R.

Atomic-scale roughness may produce still larger deviations in local quantities. Figure 3 shows the variation of the pressure P along the contact. Results for bent incommensurate crystals lie closest to the solid lines predicted by contact mechanics, showing only a small smearing at the edge of the contact. Results for a bent commensurate crystal (Fig. 3b) show sharp drops in P where atoms on the substrate and cylinder fall out of registry. The pressure on the amorphous surface shows fluctuations that are comparable to the mean, even though the results are averaged along the cylinder axis. The local pressure for the stepped surface is farthest from the prediction, because its flat terraces differ most strongly from a smooth curve. Indeed, solving the contact mechanics problem for a flat contact gives a much better description of the pressure on a stepped surface, with a minimum in the centre and singularities at the edges[1]. This, combined with previous work[9–11], suggests that continuum mechanics could be applied to smaller contacts if the true atomic-scale surface roughness was included, but such detail is seldom available and never used in practice[13].

In continuum mechanics, Saint-Venant's principle implies that changing the surface distribution of normal load on the scale of a has little effect on stresses at depths below 3a. Thus continuum predictions should grow in accuracy with increasing depth below the surface. However, the stresses are most significant at depths less than a. For example, continuum mechanics[1] predicts that the shear stress τ should peak 0.78a beneath the surface and directly below the cylinder axis. The local pressure deviations for amorphous and stepped surfaces in Fig. 3 lead to shifts in both the magnitude and location of the peaks in τ by factors of two or more. Values of the yield stress are often determined from the calculated subsurface value of τ at the onset of yield. We find that this may underestimate the yield stress by a factor of two or more because of the large local stresses below atomically rough surfaces.

Figure 4 and Supplementary Fig. S2 show that results for spherical tips with and without adhesion follow the same trends as non-adhesive cylinders. Bent crystal results with no adhesion fit well to Hertz theory. Adding adhesion produces a strongly peaked tensile ring whose location and magnitude fit the Maugis–Dugdale[20] model with independently determined values of E^* and work of adhesion w. Amorphous tips show strong fluctuations that nearly remove the tensile ring. The value of w is four times smaller than for a bent tip with the same interaction potential, and the contact radius is increased by several σ relative to continuum theory. Stepped

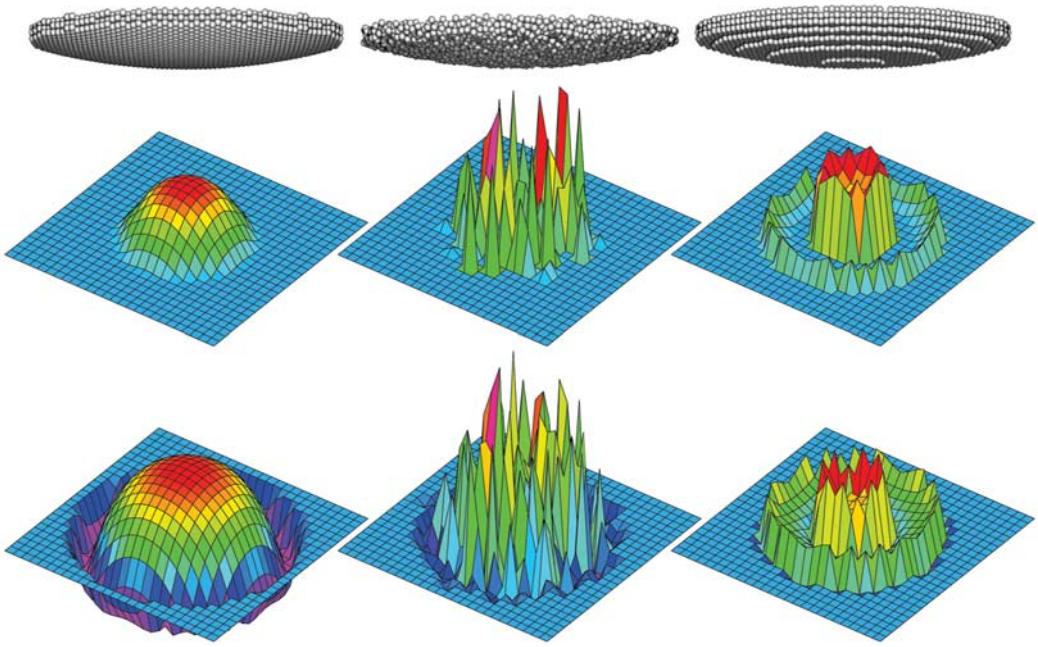

Figure 4 | Geometry and stress for spherical tips with and without adhesion. The top row shows the central regions (diameter 50σ) of bent, amorphous and stepped spherical tips, from left to right. The second and third rows show the pressure distributions for these tips with non-adhesive and adhesive interactions, respectively. In the adhesive case, the interaction potential between surfaces is about half as strong as interactions within the substrate (Supplementary Information). In all cases $N/E^*R^2 = 0.0013$ and $R = 100\sigma$. The pressure is plotted over a central square region of edge 42.9σ, with a constant vertical scale. Almost 10^7 atoms are included in the substrate to include subsurface deformations.

tips show compressive peaks at step edges that look nothing like Maugis–Dugdale predictions.

Frictional forces can also be measured with the SPM and have been used to infer a relationship between area and friction[13–16]. Analytic studies suggest that friction should be more sensitive to surface structure than other quantities[21] and this is confirmed by our simulations. Figure 2c shows the static friction F needed to initiate sliding as a function of load. The bent and cut commensurate crystal exhibit large friction forces because they can lock into local registry with the substrate[21]. Results for both can be qualitatively fitted by assuming that friction is proportional to the area predicted by contact mechanics (solid line), even though the actual area is different. Similar fits have been made to some SPM experiments where the tip is unlikely to be commensurate[13–16].

The friction for amorphous and incommensurate surfaces is much smaller (Fig. 2c) and does not scale with the contact area because the atoms cannot lock into local registry at the surface[21]. The incommensurate surface exhibits almost no friction. This is consistent with SPM measurements with crystalline tips[22,23]. The amorphous system appears to give friction proportional to load as in macroscopic friction laws[1,21]. However, we found that F/N decreases as the cylinder length l increases, as predicted for bare amorphous surfaces[21,24].

The shear modulus of materials has also been determined with SPM by measuring the stiffness resisting lateral tip displacements[13,18]. The results are analysed using continuum theory with the assumption that the surface atoms follow the tip rigidly. However, the small values of static friction for amorphous and incommensurate surfaces allow significant deviations between tip and substrate displacements. The effect is equivalent to adding another spring of stiffness of order F/σ in series with the continuum result[19]. This explains why the measured stiffness is often much less than expected[18].

We note that contact mechanics has been tested for $R > 1$ mm and $a > 1\,\mu$m where the contact area can be measured optically. However, these tests considered special cases that are consistent with our findings. Most surface force apparatus experiments[25,26] used bent mica crystals, the geometry that agrees best with continuum theory. As in Fig. 2b, a was actually slightly larger than continuum predictions, but this was attributed to systematic effects[25]. Most other experiments have considered elastomers[27–29]. While these materials are elastic at large scales, they can deform like fluids at lengths less than the cross-link spacing, allowing them to conform to atomic-scale roughness.

The above results have obvious implications for SPM experiments, suggesting that contact areas and yield stresses will be underestimated by continuum theory and that friction and contact stiffness will be overestimated. There is evidence that the same effects may apply for typical macroscopic surfaces. Statistical analyses of random rough surfaces[5,7,8,12] indicate that the typical radius of curvature R of contacting surface bumps is comparable to the smallest wavelength of height fluctuations and may be of nanometre scale. Work on quantifying these effects for complex rough surfaces is under way, and initial results show that the area may be more than twice that predicted using continuum mechanics.

Received 7 October 2004; accepted 20 April 2005.

1. Johnson, K. *Contact Mechanics* Ch. 4, 5, 13 (Cambridge Univ. Press, Cambridge, 1985).
2. Nanotechnology (special issue). *Sci. Am.* **285**(3), 32–85 (2001).
3. Bhushan, B. (ed.) *Springer Handbook of Nanotechnology* (Springer, Berlin, 2003).
4. Valiev, R. Nanomaterial advantage. *Nature* **419,** 887–889 (2002).
5. Bhushan, B., Israelachvili, J. N. & Landman, U. Nanotribology: Friction, wear and lubrication at the atomic scale. *Nature* **374,** 607–616 (1995).
6. Urbakh, M., Klafter, J., Gourdon, D. & Israelachvili, J. The nonlinear nature of friction. *Nature* **430,** 525–528 (2004).
7. Greenwood, J. A. A unified theory of surface roughness. *Proc. R. Soc. Lond. A* **393,** 133–157 (1984).
8. Hyun, S., Pei, L., Molinari, J.-F. & Robbins, M. O. Finite-element analysis of contact between elastic self-affine surfaces. *Phys. Rev. E* **70,** 026117 (2004).
9. Landman, U., Luedtke, W. D. & Gao, J. Atomic-scale issues in tribology: interfacial junctions and nano-elastohydrodynamics. *Langmuir* **12,** 4514–4528 (1996).
10. Miller, R. & Phillips, R. Critical analysis of local constitutive models for slip and decohesion. *Phil. Mag. A* **73,** 803–828 (1996).

11. Vafek, O. & Robbins, M. O. Molecular dynamics study of the stress singularity at a corner. *Phys. Rev. B* **60,** 12002–12006 (1999).
12. Persson, B. N. J. Elastoplastic contact between randomly rough surfaces. *Phys. Rev. Lett.* **87,** 116101 (2001).
13. Carpick, R. W. & Salmeron, M. Scratching the surface: fundamental investigations of tribology with atomic force microscopy. *Chem. Rev.* **97,** 1163–1194 (1997).
14. Lantz, M. A., O'Shea, S. J. & Welland, M. E. Simultaneous force and conduction measurements in atomic force microscopy. *Phys. Rev. B* **56,** 15345–15352 (1997).
15. Schwarz, U. D., Zwörner, O., Koster, P. & Wiesendanger, R. Quantitative analysis of the frictional properties of solid materials at low loads. I. Carbon compounds. *Phys. Rev. B* **56,** 6987–6996 (1997).
16. Enachescu, M. *et al.* Atomic force microscope study of an ideally hard contact: The diamond (111)/Tungsten carbide interface. *Phys. Rev. Lett.* **81,** 1877–1880 (1998).
17. Kiely, J. D. & Houston, J. E. Nanomechanical properties of Au (111), (001), and (110) surfaces. *Phys. Rev.* **B57,** 12588–12594 (1998).
18. Carpick, R. W. & Eriksson, M. A. Measurements of in-plane material properties with scanning probe microscopy. *MRS Bull.* **29,** 472–477 (2004).
19. Socoliuc, A., Bennewitz, R., Gnecco, E. & Meyer, E. Transition from stick-slip to continuous sliding in atomic friction. *Phys. Rev. Lett.* **92,** 134301 (2004).
20. Maugis, D. Adhesion of spheres: The JKR-DMT transition using a Dugdale model. *J. Colloid Interf. Sci.* **150,** 243–269 (1992).
21. Müser, M. H., Wenning, L. & Robbins, M. O. Simple microscopic theory of Amontons's laws for static friction. *Phys. Rev. Lett.* **86,** 1295–1298 (2001).
22. Hirano, M., Shinjo, K., Kaneko, R. & Murata, Y. Observation of superlubricity by scanning tunnelling microscopy. *Phys. Rev. Lett.* **78,** 1448–1451 (1997).
23. Dienwiebel, M. *et al.* Superlubricity of graphite. *Phys. Rev. Lett.* **92,** 126101 (2004).
24. Wenning, L. & Müser, M. H. Friction laws for elastic nano-scale contacts. *Europhys. Lett.* **54,** 693–699 (2001).
25. Horn, R. G., Israelachvili, J. N. & Pribac, F. Measurement of the deformation and adhesion of solids in contact. *J. Coll. Interf. Sci.* **115,** 480–492 (1987).
26. Homola, A. M., Israelachvili, J. N., McGuiggan, P. M. & Gee, M. L. Fundamental experimental studies in tribology: The transition from "interfacial" friction of undamaged molecularly smooth surfaces to "normal" friction with wear. *Wear* **136,** 65–83 (1990).
27. Maeda, N., Chen, N., Tirrell, M. A. & Israelachvili, J. N. Adhesion and friction mechanisms of polymer-on-polymer surfaces. *Science* **297,** 379–382 (2002).
28. Shull, K. R. Contact mechanics and the adhesion of soft solids. *Mater. Sci. Eng. R.* **36,** 1–45 (2002).
29. Newby, B.-m. A., Chaudhury, M. K. & Brown, H. R. Macroscopic evidence of the effect of interfacial slippage on adhesion. *Science* **269,** 1407–1409 (1995).

Supplementary Information is linked to the online version of the paper at www.nature.com/nature.

Acknowledgements We thank R. W. Carpick, J. N. Israelachvili, P. M. McGuiggan and M. H. Müser for useful discussions. This material is based upon work supported by the National Science Foundation.

Author Information Reprints and permissions information is available at npg.nature.com/reprintsandpermissions. The authors declare no competing financial interests. Correspondence and requests for materials should be addressed to M.O.R. (mr@jhu.edu).